

Article

# An Improved Wireless Battery Charging System

Woo-Seok Lee <sup>1</sup>, Jin-Hak Kim <sup>1</sup>, Shin-Young Cho <sup>2</sup> and Il-Oun Lee <sup>1,\*</sup> 

<sup>1</sup> Department of Electrical Engineering, Myongji University, Yongin 17058, Korea; a5883283@naver.com (W.-S.L.); suwxz@naver.com (J.-H.K.)

<sup>2</sup> Agency for Defense Development, Daejeon 34186, Korea; martin@kaist.ac.kr

\* Correspondence: leeiloun@mju.ac.kr; Tel.: +82-31-330-6833

Received: 12 March 2018; Accepted: 27 March 2018; Published: 29 March 2018



**Abstract:** This paper presents a direct wireless battery charging system. The output current of the series-series compensated wireless power transfer (SS-WPT) system is used as a current source, and the output voltage of AC-DC converter controls the current source. Therefore, the proposed wireless battery charging system needs no battery charging circuit to carry out charging profiles, and can solve space constraints and thermal problems in many battery applications. In addition, the proposed wireless battery charging system can implement easily most other charging profiles. In this paper, the proposed wireless battery charging system is implemented and the feasibility is verified experimentally according to constant-current constant-voltage charging profile or multi-step current charging profile.

**Keywords:** wireless battery charging system; wireless power transfer; series-series compensated circuit

## 1. Introduction

The use of portable electronic devices and electric vehicles has become more widespread recently, the many electronic devices and electronic vehicles are plugged into wall outlets via power cables for many hours a day, and the use of wired charging apparatuses has become a part of daily life. In this scenario, a large number of wire-chargers are discarded as E (electronics)-waste due to contact failures such as broken wires or short-circuit problems, etc. Due to the increasing E (electronic)-waste problem, there has been increasing interest in the study and development of wireless power transfer (WPT) technology that can be utilized to transfer power to batteries without requiring expensive failure-prone connectors.

WPT technology can provide charging systems with low maintenance costs, high reliability, and the ability to operate even in extreme environments [1]. However, a wireless battery charging system requires more power stages than a wired battery charging system [2,3]. The wireless battery charging system needs a WPT system that consists of a power transmitter and a power receiver. An exclusive controller is also required to regulate the output of WPT system since the power transferred to the receiver of WPT system is not regulated whenever the load changes. The inverter or converter in power electronics is usually controlled by three methods; pulse width modulation (PWM), frequency modulation (FM), and amplitude modulation (AM). The AM method requires an additional stage for the DC-DC converter in order to control the amplitude of the input voltage. On the other hand, both PWM and FM need no additional stage since the inverter or converter uses power semiconductor switches for the power conversion. For this reason, when PWM or FM is applied to the power transmitter of a WPT system, the power transferred to the receiver can be easily regulated. Nevertheless, high current stress and large power loss are generated since the voltage and current in the power transmitter are not in phase. Due to this problem, regulation circuits such as

synchronous rectifiers [2,3] or impedance tuners [4] are necessary in the receiver of a WPT system. Furthermore, battery-charging circuits such as low-dropout (LDO) regulators [2,3] or synchronous buck converters [4] are required for the battery charging. Figure 1 shows a conventional wireless battery charging system. As mentioned above, the conventional system consists of the following five key power stages; AC-DC converter, power transmitter of WPT system, power receiver of WPT system, regulation circuit, and battery-charging circuit.

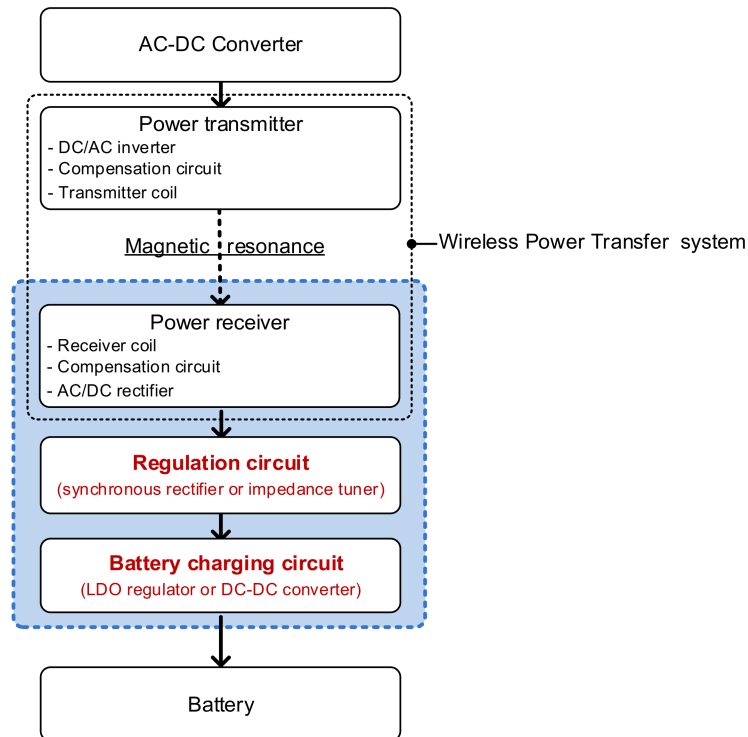


Figure 1. Conventional wireless battery charging system.

For the wireless battery charging system, the power receiver, regulation circuit, and battery charging circuit must be embedded inside portable electronic devices or electric vehicles, but there is usually not enough space for these power stages. In addition to this problem, the regulation and battery-charging circuits generate huge heat and raise the problem of thermal stress on the electronic devices while being charged.

In this paper, a direct wireless battery charging system is proposed. The regulation and battery charging circuits in the conventional wireless battery charging system are removed, and the battery is charged directly from WPT system. Figure 2 shows the proposed direct wireless battery charging system. As shown in Figure 2, the proposed system is only made of AC-DC converter, power transmitter, and power receiver. The type of the applied WPT system is a series-series compensated wireless power transfer (SS-WPT) system, and it is connected directly to the battery. Generally, the output of SS-WPT system has inherent characteristic as a current source. Hence, without the help of dedicated regulation and battery charging circuits, the battery can be charged directly from the WPT system by adjusting the output voltage of the existing AC-DC converter in front of the WPT system according to the constant-current constant-voltage (CC-CV) charging profile [5–11] or a multi-step current charging profile [12–18].

The paper is organized as follows: in Section 2, the inherent current-source characteristics of the SS-WPT system are described. The implementation of the CC-CV charging or MCC charging profile in the proposed wireless battery charging system is explained in Section 3. Experimental verification is presented in Section 4, and finally, Section 5 draws the conclusions.

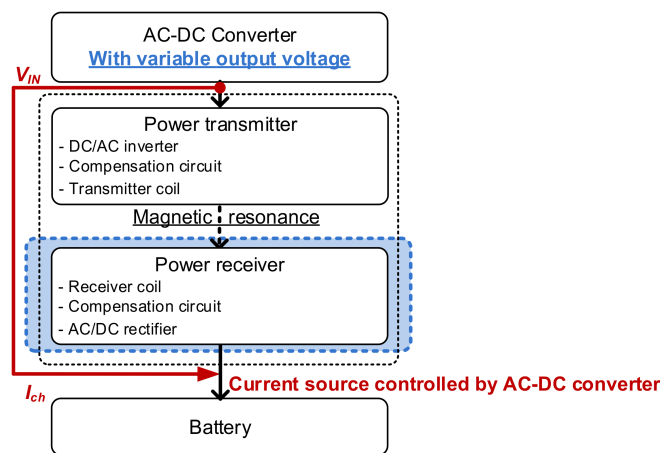


Figure 2. Proposed wireless battery charging system.

## 2. Current Source Characteristic of Series-Series Compensated Wireless Power Transfer

In the proposed wireless battery charging system, the SS-WPT system followed by AC-DC converter consists of a half-bridge inverter, resonant tank, full-bridge rectifier, filter, and load as the battery, as shown in Figure 3. The half-bridge inverter applies a square voltage into the resonant tank. The square voltage,  $V_{square}$  can be described as:

$$V_{square}(t) = \begin{cases} V_{IN} & (0 < \omega t \leq \pi) \\ 0 & (\pi < \omega t \leq 2\pi) \end{cases} \quad (1)$$

where  $\omega = 2\pi f_S$  and  $f_S$  is the switching frequency of the half-bridge inverter in Figure 3.

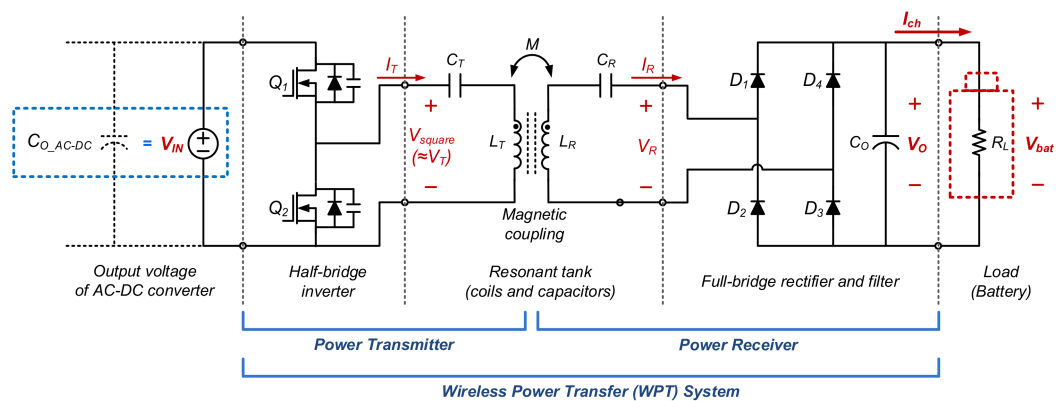


Figure 3. Series-series compensated wireless power transfer circuit in the proposed system.

The resonant tank consists of a transmitter coil, receiver coil, transmitter capacitor, and receiver capacitor. The capacitors in the resonant tank resonate with coils and improve the conversion efficiency of the system. Since the capacitors are in series with coils, the structure is called series-series (SS) compensation [19,20]. Since the series-series compensated resonant tank acts as a band pass filter, the effect of any harmonic components in the input square voltage  $V_{square}$  can be neglected, except for its fundamental component. Then, the transmitter and receiver voltages in the resonant tank are sinusoidal and expressed as  $V_T$  and  $V_R$ , respectively. The transmitter and receiver currents are also

sinusoidal and expressed as  $I_T$  and  $I_R$ , respectively. The load represented as  $R_L$  can be described with an equivalent load resistance  $R_{eq}$  [20]:

$$R_{eq} = \frac{8}{\pi^2} R_L \tag{2}$$

Figure 4a shows the equivalent circuit of the SS-WPT system in Figure 3, which consists of a sinusoidal transmitter voltage  $V_T$ , capacitors, a coupled-inductor model, and an equivalent load resistance  $R_{eq}$ . The components in the receiver side can be transformed into the transmitter side by the effective transformer turns-ratio,  $n$ . Here, the term  $n$  can be expressed as:

$$n = \sqrt{L_T/L_R} \tag{3}$$

where  $L_T$  and  $L_R$  are the transmitter coil's self-inductance and receiver coil's self-inductance, respectively.

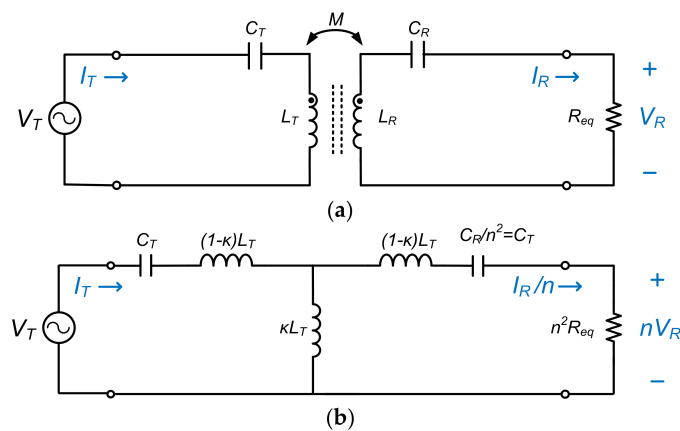


**Figure 4.** Equivalent circuits of series-series compensated wireless power transfer system: (a) equivalent circuit and (b) modified equivalent circuit.

The modified equivalent circuit of SS-WPT system can be represented with coupling coefficient  $\kappa$ ,  $L_T$ , and  $C_T$  as shown in Figure 4b, assuming  $n = 1$  and  $C_T = C_R$ . Figure 5 shows the modified equivalent circuit of SS-WPT system in frequency-domain.

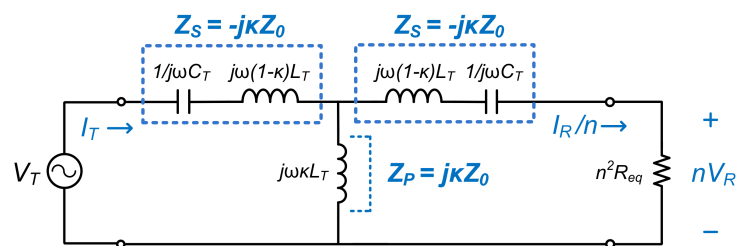


**Figure 5.** Equivalent circuit of series-series compensated wireless power transfer system in frequency domain.

The series impedance  $Z_S$  and parallel impedance  $Z_P$  are expressed as:

$$Z_S = j\omega L_T \left(1 - \frac{\omega^2}{\omega_r^2}\right) - j\kappa\omega L_T = -j\kappa\omega_r L_T = -j\kappa Z_0 \text{ and} \tag{4}$$

$$Z_P = j\kappa\omega L_T = j\kappa\omega_r L_T = j\kappa Z_0 \tag{5}$$

where  $\omega_r$  is the resonant angular frequency and  $Z_O$  is the characteristic impedance. The series impedance  $Z_S$  and parallel impedance  $Z_P$  have the same magnitude, but different phase. To define the characteristics between input and output parameters, the resonant tank can be described as the transmission matrix in Equation (6). From Equation (6), the relationship between input and output parameters can be obtained in as Equation (7):

$$\begin{bmatrix} V_T \\ I_T \end{bmatrix} = \begin{bmatrix} 0 & -j\kappa Z_O \\ -j\frac{1}{\kappa Z_O} & 0 \end{bmatrix} \begin{bmatrix} nV_R \\ I_R/n \end{bmatrix} \quad (6)$$

$$V_T = -j\kappa Z_O I_R/n \text{ and } I_T = -j\kappa \frac{1}{Z_O} nV_R \quad (7)$$

In Equation (7), it is known that the sinusoidal receiver current  $I_R$  is proportional to the sinusoidal transmitter voltage  $V_T$ . This means that SS-WPT system driven by the fixed output voltage of AC-DC converter behaves as a constant current-source. In addition, if the magnitude of the output voltage of AC-DC converter is controlled, the SS-WPT system is able to be a voltage controlled current-source at the resonant frequency. From Equation (7), the battery charging current,  $I_{ch}$  of the SS-WPT system in Figure 3 can be described with the input voltage  $V_{IN}$  as follows:

$$I_{ch} = \frac{4}{\pi^2} \cdot \frac{nV_{IN}}{\kappa Z_O} \quad (8)$$

Then, the output voltage  $V_O$  can be expressed with the  $I_{ch}$  as in Equation (9):

$$V_O = I_{ch} R_L = \frac{4}{\pi^2} \cdot \frac{nV_{IN}}{\kappa Z_O} R_L \quad (9)$$

Since the output voltage  $V_O$  of SS-WPT system is clamped at the battery voltage  $V_{bat}$ , the load resistance  $R_L$  can be determined from the  $V_{bat}$  and  $I_{ch}$ :

$$R_L = \frac{V_{bat}}{I_{ch}} \quad (10)$$

### 3. Implementation of CC-CV and MCC Charging

When the battery is not charged, it can be approximately modeled as only a capacitor with a high capacitance. At this state, the battery voltage  $V_{bat}$  is called open circuit voltage  $V_{OC}$ . On the other hand, when the battery is charged by the charging current  $I_{ch}$ , the battery voltage  $V_{bat}$  is called closed circuit voltage  $V_{CC}$ , which is lower than  $V_{OC}$  due to the IR voltage drop  $V_\eta$  across the overpotential resistance  $R_\eta$  and the voltage drop  $V_P$  by polarization. The relationship between  $V_{OC}$  and  $V_{CC}$  can be expressed as:

$$V_{CC} = V_{OC} + V_\eta + V_P \quad (11)$$

In order to charge the battery fully, the open circuit voltage  $V_{OC}$  should be able to arrive at the maximum allowable battery voltage  $V_{max\_bat}$ . However, although the  $V_{CC}$  observed externally while being charged can reach to the  $V_{max\_bat}$ , the  $V_{OC}$  is always lower than the  $V_{max\_bat}$  due to the two voltage drops in Equation (11). To solve this, the charging current  $I_{ch}$  should be reduced to a predetermined small value  $I_{sm}$  at the end-of-charge because the  $V_\eta$  and  $V_P$  are proportional to the  $I_{ch}$ .

#### 3.1. CC-CV Charging Profile

Figure 6a shows the concept on implementation of constant-current and constant-voltage charging in the proposed system. On the CC phase of the CC-CV charging, the relative high current is required for  $I_{ch}$  for the fast charge. Since the charging current  $I_{ch}$  of SS-WPT system is proportional to the input voltage  $V_{IN}$  as in Equation (8), this means that the output voltage of AC-DC converter in the proposed wireless

charging system (or  $V_{IN}$ ) must be set high. According to this principle, a fixed high  $V_{IN}$  is required for a constant high  $I_{ch}$  in the proposed system and then, the  $I_{ch}$  will charge the battery directly until the closed circuit voltage  $V_{CC}$  reaches the maximum allowable battery voltage  $V_{max\_bat}$ , as shown in Figure 6a.

On the CV phase, the  $I_{ch}$  begins to decreasing and the decreasing  $I_{ch}$  reduces the two voltage drops of  $V_{\eta}$  and  $V_P$  to allow the open circuit voltage  $V_{OC}$  to reach the maximum allowable battery voltage  $V_{max\_bat}$ . At the end of CV phase, the  $I_{ch}$  reaches the predetermined small current  $I_{sm}$ . For this mechanism, the proposed system must reduce the output voltage of AC-DC converter on CV phase. As a result, the  $I_{ch}$  of SS-WPT system will decrease and the open circuit voltage  $V_{OC}$  will continue to increase. The two voltage drops  $V_{\eta}$  and  $V_P$  will decrease gradually on the CV phase. On the other hand, the closed circuit voltage  $V_{OC}$  will be hold at the maximum allowable battery voltage  $V_{max\_bat}$  due to the constant sum of the increased open circuit voltage  $V_{OC}$  and the decreased two voltage drops  $V_{\eta}$  and  $V_P$ .

When CC-CV charging is implemented in the conventional system, any transient phase may occur during the switching time from CC control mode to CV control mode [7]. However, in the proposed wireless battery charging system, the current source characteristic of SS-WPT system is used on the CC phase and only the voltage feedback loop is required on the CV phase. This means that in the proposed system, the CC phase is always switched into the CV phase smoothly.

### 3.2. MCC Charging Profile

Figure 6b shows the concept on implementation of multi-current charging in the proposed system. The MCC charging is composed of various CC phases with different constant magnitudes for  $I_{ch}$ . In this profile, whenever the closed circuit voltage  $V_{CC}$  reaches the predetermined voltage  $V_{pre\_bat}$ , the charging currents  $I_{ch}$  is stepped down in turn. On the last CC phase of the MCC charging, the  $I_{ch}$  should be stepped down to the predetermined small current  $I_{sm}$  to charge the battery fully, as shown in Figure 6b. In the proposed wireless battery charging system, this mechanism can be implemented by stepping down the output voltage of AC-DC converter in turn according to the MCC charging profile.

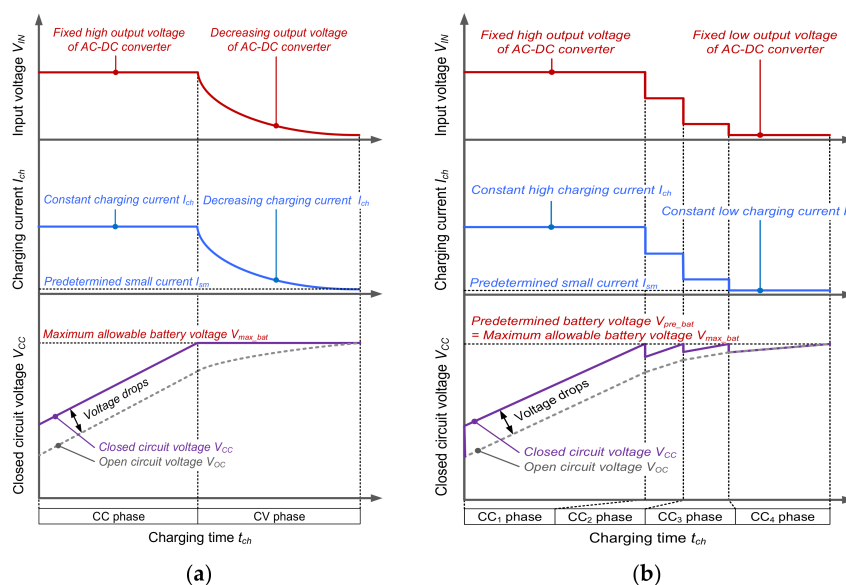


**Figure 6.** Concept on implementation of (a) constant-current and constant-voltage charging and (b) four-step CC charging with step-down charging current (when the predetermined battery voltage is the maximum allowable battery voltage) profiles in the proposed system.

### 3.3. Other Charging Profile

The battery is charged generally from one current source, and the battery charging circuit carries out the role of the current source in the conventional wireless charging system. On the other hand,

the SS-WPT system is used as a current source for the battery charging in the proposed wireless charging system. The current-level of the current source by the SS-WPT can be adjusted variously by changing the output voltage of AC-DC converter, as analyzed in Equation (8). From this, it is noted that most other charging techniques such as constant power charging [21–24], boost charging [25], varying current decay [26], and optimal charging based on temperature rise and charge time [27] can be implemented easily by the use of the proposed system.

## 4. Experimental Verification

### 4.1. Experimental Conditions

A prototype was made to verify the proposed wireless battery charging system. Symmetric wire-wound spiral coils (inner diameter: 30 mm and outer diameter: 70 mm) with ferrite sheet (width: 90 mm, length: 75 mm, and height: 500  $\mu\text{m}$ ) are fabricated as illustrated in Figure 7. Symmetric wire-wound spiral coils are separated by the air gap of 15 mm. The thickness of transmitter case is 1 mm, and the thickness of receiver case is 1 mm. The parameters in Figure 3 for the experiment are listed in Table 1.

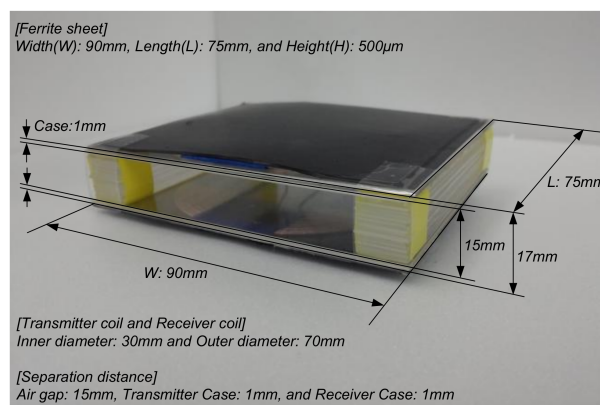


Figure 7. Symmetric wire-wound spiral coils with ferrite sheet.

Table 1. Parameters for experiments.

Symbol	Description	Values/Part Name
$L_T$	Self-inductance of transmitter coil	50 $\mu\text{H}$
$L_R$	Self-inductance of receiver coil	50 $\mu\text{H}$
$\kappa$	Coupling coefficient	0.4
$n$	Turns-ratio	1 (27:27)
$C_T$	Transmitter capacitance	78 nF
$C_R$	Receiver capacitance	78 nF
$Q_1, Q_2$	Switches	50CN10N
$D_1-D_4$	Diodes	PMEG4030ER
$f_r$	Resonant frequency	80 kHz

The lithium-ion batteries used for the experiment are prismatic 3100 mAh batteries (Samsung, city, country) which have the minimum allowable battery voltage  $V_{min\_bat}$  of 3.4 V and a maximum allowable battery voltage  $V_{max\_bat}$  of 4.3 V. One battery is charged according to the CC-CV charging profile, and another battery is charged based on the MCC charging profile. The input voltage  $V_{IN}$ , the charging current  $I_{ch}$ , and the closed circuit voltage  $V_{CC}$  are simultaneously recorded by a MV1000 digital recorder (Yokogawa, Japan).

Figure 8 shows the measured  $I_{ch}$  by changing the input voltage  $V_{IN}$  of SS-WPT system. As shown in Figure 8, the charging current  $I_{ch}$  of the proposed system increases linearly from 100 mA to 1000 mA when adjusting the  $V_{IN}$  from 3.61 V to 27.46 V. From this result, it is confirmed that the SS-WPT system

behaves as a voltage controlled current source at the resonant frequency. The voltage controlled current source will charge the two batteries from the minimum allowable battery voltage  $V_{min\_bat}$  of 3.4 V to the maximum allowable battery voltage  $V_{max\_bat}$  of 4.3 V. And the  $I_{ch}$  at the end of CV phase is set to the predetermined small current  $I_{sm}$  of 100 mA.

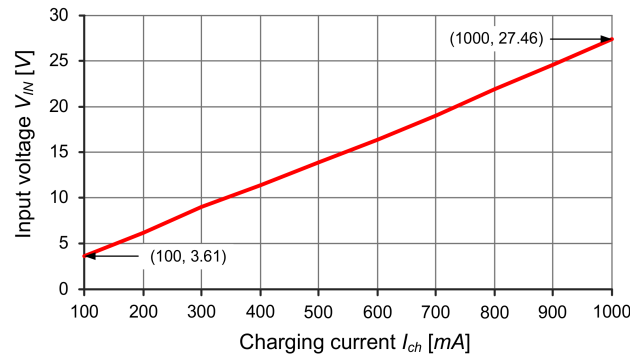


**Figure 8.** Measured relationship between input voltage and charging current in series-series compensated wireless power transfer system.

#### 4.2. CC and CV Charging Profile

Figure 9 shows the measured curves of CC-CV charging in the proposed system. The input voltage  $V_{IN}$  is set at 27.46 V to obtain the charging current  $I_{ch}$  of 1000 mA on the CC phase. Then, the  $I_{ch}$  of 1000 mA starts to charge the battery. The closed circuit voltage  $V_{CC}$  increases sharply due to the two voltage drops of  $V_{\eta}$  and  $V_P$  at the start point of the CC phase, and then reaches the maximum allowable battery voltage  $V_{max\_bat}$  of 4.3 V from 3.9 V, as shown in Figure 9. Figure 10 shows the measured key waveforms in the SS-WPT system while the closed circuit voltage  $V_{CC}$  moves from 3.9 V to 4.3 V. As shown in Figure 10, the key waveforms at the  $V_{CC}$  of 3.9 V is nearly similar to that at 4.3 V. At the end of CC phase, the  $V_{CC}$  reaches the  $V_{max\_bat}$  of 4.3 V, but the open circuit voltage  $V_{OC}$  will be not 4.3 V due to the two voltage drops  $V_{\eta}$  and  $V_P$ .

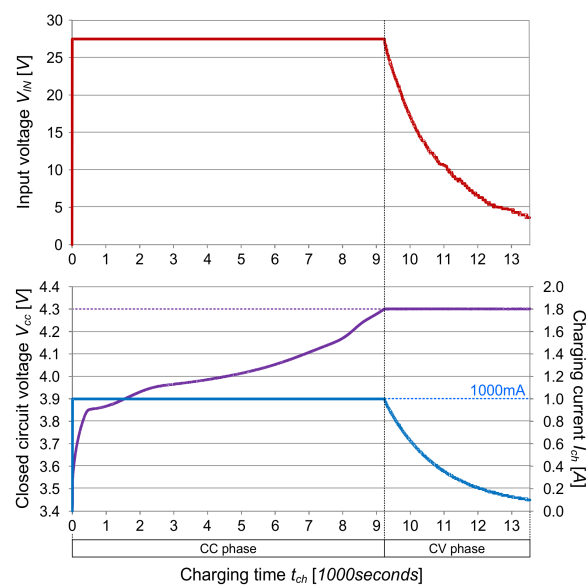


**Figure 9.** Measured curves of CC-CV charging in the proposed wireless battery charging method.

On the CV phase after the CC phase, the  $I_{ch}$  is decreased by reducing the  $V_{IN}$  in order to charge the battery fully. Then, the two voltage drops of  $V_{\eta}$  and  $V_P$  is reduced and the open circuit voltage



$V_{OC}$  of the battery will arrive at the  $V_{max\_bat}$  of 4.3 V. Figure 11 shows the key waveforms in SS-WPT system on the CV phase. Since the WPT system operates at the resonant frequency, the input square voltage  $V_{square}$  and the transmitter resonant current  $I_T$  are almost in phase. Also, the receiver resonant current  $I_R$  leads the  $I_T$  by about  $\pi/2$ . When the  $I_{ch}$  reaches the predetermined small current  $I_{sm}$  of 100 mA, the CC-CV charging profile ends. The total charging time  $t_{ch}$  is 13,540 s.

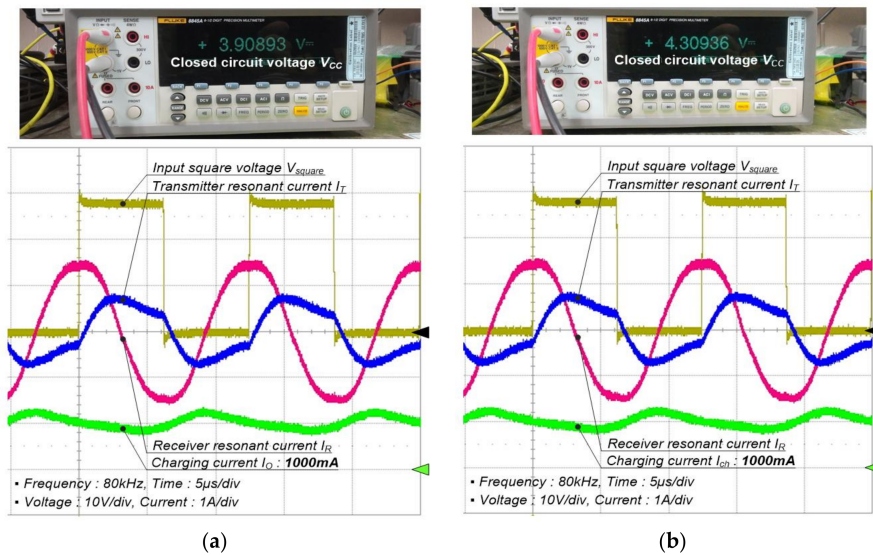


**Figure 10.** Key waveforms of series-series compensated wireless power transfer system in constant-current phase: (a) closed circuit voltage of 3.9 V and load resistance 3.9 Ω at the middle of constant-current phase and (b) closed circuit voltage of 4.3 V and load resistance 4.3 Ω at the end of constant-current phase.

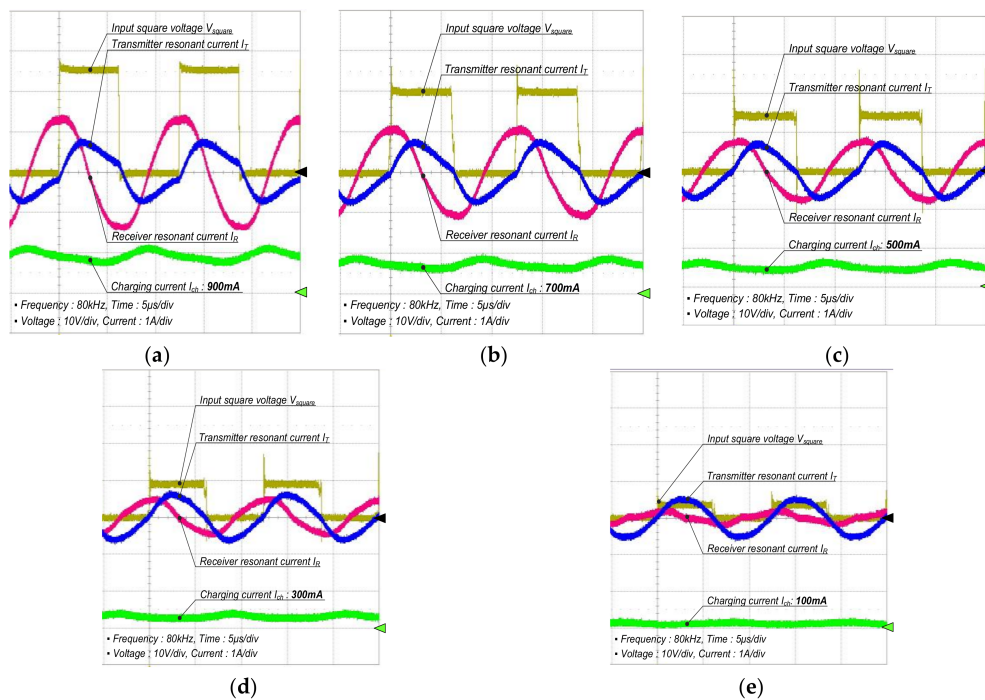


**Figure 11.** Key waveforms of series-series compensated wireless power transfer system in constant-voltage phase: (a) charging current of 900 mA, (b) charging current of 700 mA, (c) charging current of 500 mA, (d) charging current of 300 mA, and (e) charging current of 100 mA.

Concretely, the charging times on the CC phase is 9238 s and the CV phase needs a time of 4302 s. With this experiment, it is also confirmed that the total charging time  $t_{ch}$  measured in the proposed wireless battery charging system is almost equal to that of the conventional wired battery charging system (13,200 s) under the same conditions.

#### 4.3. MCC Charging Profile

Another battery is charged according to the MCC charging profile consisting of four CC phases. Figure 12 shows the measured curves of MCC charging in the proposed system. While charging the battery, the constant charging current  $I_{ch}$  is stepped down as follows: CC<sub>1</sub> phase (1000 mA)–CC<sub>2</sub> phase (800 mA)–CC<sub>3</sub> phase (600 mA)–CC<sub>4</sub> phase (400 mA)–CC<sub>5</sub> phase (100 mA), as shown in Figure 12. The  $I_{ch}$  on the last CC phase is set to the predetermined small current  $I_{sm}$  of 100 mA to charge the battery fully. The output voltage of AC-DC converter is stepped down to 27.46 V, 22.06 V, 16.38 V, 11.39 V, and 3.61 V in sequence in order to obtain the constant  $I_{ch}$  of 1000 mA, 800 mA, 600 mA, 400 mA, and 100 mA, respectively.

The maximum allowable battery voltage  $V_{max\_bat}$  is selected as the predetermined battery voltage  $V_{pre\_bat}$ . As a result, when the closed circuit voltage  $V_{CC}$  reaches the  $V_{max\_bat}$  of 4.3 V, the  $I_{ch}$  are stepped down as shown in Figure 12. The total charging time  $t_{ch}$  under this MCC charging condition is 16,892 s.

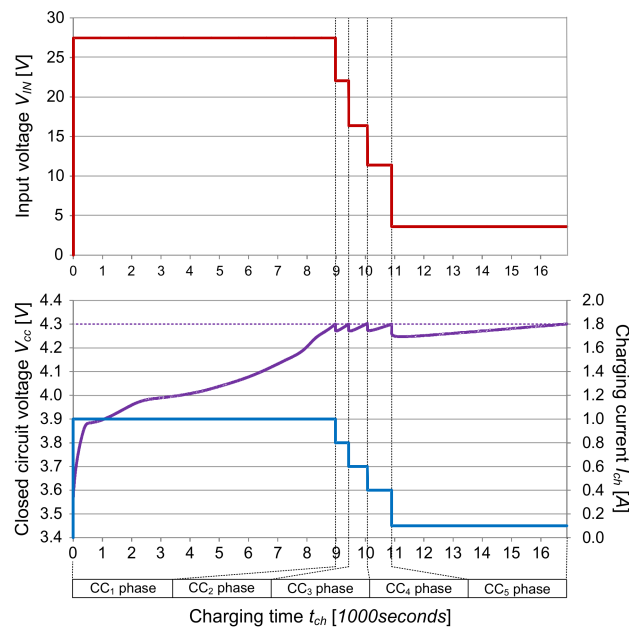


**Figure 12.** Measured curves of MCC charging in the proposed wireless battery charging method.

## 5. Conclusions

This paper proposes a direct wireless battery charging system. Since the proposed system takes advantage of the inherent current-source characteristic of SS-WPT system, the regulation and battery-charging circuits in the conventional system are eliminated and hence it can be easily implemented in many battery applications such as portable electronic devices and electric vehicles, etc. In addition, a voltage controlled current source implemented by changing the output voltage of AC-DC converter in the proposed system can directly charge the battery. This enables us to easily implement various battery charging profiles such as CC-CV, MCC, etc. without an exclusive current feedback loop. In this paper, the abovementioned merits of the proposed system were analyzed in detail and the feasibility was verified with experiments based on a prototype of the proposed system, using Samsung prismatic 3100 mAh lithium-ion batteries, and a CC-CV charging profile. From the results, it can be stated that the proposed system will be more competitive than the conventional system.

**Acknowledgments:** This work was supported by “Human Resources Program in Energy Technology” of the Korea Institute of Energy Technology Evaluation and Planning (KETEP), granted financial resource from the Ministry of Trade, Industry & Energy, Republic of Korea. (No. 20174030201790). This research was supported by Basic Science Research Program through the National Research Foundation of Korea (NRF) funded by the Ministry of Science, ICT & Future Planning (2015R1C1A1A01051992).

**Author Contributions:** Il-Oun Lee and Shin-Young Cho were the main researchers who initiated and organized research reported in the paper, all authors including Woo-Seok Lee were responsible for making the prototype of the proposed system and carrying out the experiment.

**Conflicts of Interest:** The authors declare not conflict of interest.

## References

- Jiang, H.; Brazis, P.; Tabaddor, M.; Bablo, J. Safety considerations of wireless charger for electric vehicles—A review paper. In Proceedings of the 2012 IEEE Symposium on Product Compliance Engineering Proceedings, Portland, OR, USA, 5–7 November 2012.
- Why Not A Wire? The Case for Wireless Power, Texas Instruments. Available online: <http://www.wirelesspowerconsortium.com/technology/why-not-a-wire-the-case-for-wireless-power.html> (accessed on 28 March 2018).
- Texas Instruments (TI), “bq51050B and bq51051B Datasheet”. Available online: <http://www.ti.com/lit/ds/symlink/bq51050b.pdf> (accessed on 28 March 2018); Linear Technology, “LTC4120 Datasheet”. Available online: <http://cds.linear.com/docs/en/datasheet/4120fa.pdf> (accessed on 28 March 2018).
- Li, P.; Bashirullah, R. A Wireless Power Interface for Rechargeable Battery Operated Medical Implants. *IEEE Trans. Circuits Syst. II* **2007**, *54*, 912–916. [CrossRef]
- Dearborn, S. Charging Li-ion batteries for maximum run times. *Power Electron. Technol.* **2005**, *40*–49. Available online: [www.powerelectronics.com](http://www.powerelectronics.com) (accessed on 28 March 2018).
- Chen, M.; Rincón-Mora, G.A. Accurate, Compact, and Power-Efficient Li-Ion Battery Charger Circuit. *IEEE Trans. Circuits Syst. II* **2006**, *53*, 1180–1184. [CrossRef]
- Lin, C.-H.; Hsieh, C.-Y.; Chen, K.-H. A Li-Ion Battery Charger with Smooth Control Circuit and Built-In Resistance Compensator for Achieving Stable and Fast Charging. *IEEE Trans. Circuits Syst. I Regul. Pap.* **2010**, *57*, 506–517.
- Bruno, D.V.; Wentz, C.T.; Sarpeshkar, R. An Area and Power-Efficient Analog Li-Ion Battery Charger Circuit. *IEEE Trans. Biomed. Circuits Syst.* **2011**, *5*, 131–137.
- Inoa, E.; Wang, J. PHEV Charging Strategies for Maximized Energy Saving. *IEEE Trans. Veh. Technol.* **2011**, *60*, 2978–2986. [CrossRef]
- Chen, B.-Y.; Lai, Y.-S. New digital-controlled technique for battery charger with constant current and voltage control without current feedback. *IEEE Trans. Ind. Electron.* **2012**, *59*, 1545–1553. [CrossRef]
- Liu, Y.-H.; Teng, J.-H.; Lin, Y.-C. Search for an optimal rapid charging pattern for lithium-ion batteries using ant colony system algorithm. *IEEE Trans. Ind. Electron.* **2005**, *52*, 1328–1336. [CrossRef]
- Ikeya, T.; Iwasaki, M.; Takagi, S.; Sugii, Y.; Yada, M.; Sakabe, T.; Kousaka, E.; Tsuchiya, H.; Kanetsuki, M.; Nasu, H.; et al. Collaborative investigation on charging electric-vehicle battery systems for night-time load levelling by Japanese electric power companies. *J. Power Sources* **1997**, *69*, 103–111. [CrossRef]
- Ikeya, T.; Sawada, N.; Takagi, S.; Murakami, J.-I.; Kobayashi, K.; Sakabe, T.; Kousaka, E.; Yoshioka, H.; Katoh, S.; Yamashita, M.; et al. Multi-step constant-current charging method for electric vehicle, valve-regulated, lead/acid batteries during night time for load-levelling. *J. Power Sources* **1998**, *75*, 101–107. [CrossRef]
- Ikeya, T.; Sawada, N.; Takagi, S.; Murakami, J.-I.; Kobayashi, K.; Sakabe, T.; Kousaka, E.; Yoshioka, H.; Kato, S.; Yamashita, M.; et al. Charging operation with high energy efficiency for electric vehicle valve-regulated lead-acid battery system. *J. Power Sources* **2000**, *91*, 130–136. [CrossRef]
- Ikeya, T.; Sawada, N.; Murakami, J.-I.; Kobayashi, K.; Hattori, M.; Murotani, N.; Ujiie, S.; Kajiyama, K.; Nasu, H.; Narisoko, H.; et al. Multi-step constant-current charging method for an electric vehicle nickel/metal hydride battery with high-energy efficiency and long cycle life. *J. Power Sources* **2002**, *105*, 6–12. [CrossRef]
- Liu, Y.-H.; Hsieh, C.-H.; Luo, Y.-F. Search for an Optimal Five-Step Charging Pattern for Li-Ion Batteries Using Consecutive Orthogonal Arrays. *IEEE Trans. Energy Convers.* **2011**, *26*, 654–661. [CrossRef]

17. Liu, Y.-H.; Luo, Y.-F. Search for an Optimal Rapid-Charging Pattern for Li-Ion Batteries Using the Taguchi Approach. *IEEE Trans. Ind. Electron.* **2010**, *57*, 3963–3971. [[CrossRef](#)]
18. Wang, C.-S.; Covic, G.A.; Stielau, O.H. Power transfer capability and bifurcation phenomena of loosely coupled inductive power transfer systems. *IEEE Trans. Ind. Electron.* **2004**, *51*, 148–157. [[CrossRef](#)]
19. Moradewicz, A.J.; Kazmierkowski, M.P. Contactless energy transfer system with FPGA-controlled resonant converter. *IEEE Trans. Ind. Electron.* **2010**, *57*, 3181–3190. [[CrossRef](#)]
20. Steigerwald, L. A comparison of Half-Bridge Resonant Converters. *IEEE Trans. Power Electron.* **1988**, *3*, 174–182. [[CrossRef](#)]
21. Poon, N.K.; Pong, B.M.H.; Tse, C.K. A constant-power battery charger with inherent soft switching and power factor correction. *IEEE Trans. Power Electron.* **2003**, *18*, 1262–1269. [[CrossRef](#)]
22. Yan, X.; Patterson, D. A high-efficiency on-board battery charger with unity input power factor. *Int. J. Renew. Energy Eng.* **2000**, *2*, 141–147.
23. Kuperman, A.; Levy, U.; Goren, J.; Zafransky, A.; Savernin, A. Battery Charger for Electric Vehicle Traction Battery Switch Station. *IEEE Trans. Ind. Electron.* **2013**, *60*, 5391–5399. [[CrossRef](#)]
24. Notten, P.H.L.; Veld, J.H.G.; van Beek, J.R.G. Boost charging Li-ion batteries: A challenging new charging concept. *J. Power Sources* **2005**, *145*, 89–94. [[CrossRef](#)]
25. Chung, S.K.; Andriiko, A.A.; Mon'ko, A.P.; Lee, S.H. On charge conditions for Li-ion and other secondary lithium batteries with solid intercalation electrodes. *J. Power Sources* **1999**, *79*, 205–211. [[CrossRef](#)]
26. Sikha, G.; Ramadass, P.; Haran, B.S.; White, R.E.; Popov, B.N. Comparison of the capacity fade of Sony US 18650 cells charged with different protocols. *J. Power Sources* **2003**, *122*, 67–76. [[CrossRef](#)]
27. Zhang, C.; Jiang, J.; Gao, Y.; Zhang, W.; Liu, Q.; Hu, X. Charging optimization in lithium-ion batteries based on temperature rise and charge time. *Appl. Energy* **2017**, *194*, 569–577. [[CrossRef](#)]



© 2018 by the authors. Licensee MDPI, Basel, Switzerland. This article is an open access article distributed under the terms and conditions of the Creative Commons Attribution (CC BY) license (<http://creativecommons.org/licenses/by/4.0/>).